RSC Advances

PAPER

View Article Online
View Journal | View Issue

Cite this: *RSC Adv.*, 2026, **16**, 23637

Oleuropein derived from olive leaves inhibits the activity of *Helicobacter pylori* urease: network pharmacology, inhibition kinetics, and mechanistic insights

Luyou Zhao,[a] Haohui Chen,[a] Dandan Zheng,[b] Jingjing Wu,[a] Lin Tan,[a] Qiang Lu*[a] and Cailan Li *[bcd]

Oleuropein, the major bioactive secoiridoid in olive leaves, has been reported to exhibit anti-*Helicobacter pylori* (*H. pylori*) activity. However, its precise molecular targets and the underlying mechanisms, especially its direct interactions with key virulence factors, remain poorly defined. This study aimed to elucidate the inhibitory effect and mechanism of oleuropein on a crude *H. pylori* urease (HPU) extract using jack bean urease (JBU) as a reference enzyme and by integrating network pharmacology-based target prediction with comprehensive experimental validation. Network pharmacology analysis identified urease subunits within a key functional module of the *H. pylori* protein–protein interaction network, suggesting urease as a high-priority target of oleuropein. Subsequent enzymatic assays showed that oleuropein inhibited both HPU and JBU activities in a concentration-dependent manner, exhibiting IC_{50} values of 1.27 ± 0.04 mM and 2.17 ± 0.03 mM, respectively. Kinetic analyses indicated that oleuropein acts as a slow-binding, mixed-type inhibitor of HPU activity and a slow-binding, noncompetitive inhibitor of JBU activity, revealing distinct interaction patterns with bacterial and plant ureases. Protection and reactivation experiments using thiol-containing reagents demonstrated that the inhibition is reversible and involves interaction with sulfhydryl groups at the active site of urease. Consistent with these findings, molecular docking results suggested that oleuropein binds in the vicinity of the flap region of HPU and forms stabilizing hydrogen bonds and hydrophobic interactions with key residues, including CYS321, which is critical for maintaining active-site conformation. In conclusion, this study provides the first systematic evidence that oleuropein acts as an effective, reversible, and slow-binding inhibitor of HPU activity, possibly involving interactions with thiol-containing residues at or near the enzyme's active site. These findings offer a mechanistic explanation for the anti-*H. pylori* effects of oleuropein and support its potential as a natural lead compound for the development of urease-targeted interventions against *H. pylori*-associated gastrointestinal diseases.

Received 16th January 2026
Accepted 21st April 2026

DOI: 10.1039/d6ra00410e

rsc.li/rsc-advances

1. Introduction

Helicobacter pylori (*H. pylori*), a Gram-negative bacterium, first identified by Warren and Marshall in 1982, is a significant pathogen responsible for chronic gastritis, peptic ulcer disease, and gastric mucosa-associated lymphoid tissue disorders.[1,2] It is estimated that half of the world's population is infected with *H. pylori*, with a higher prevalence in developing regions.[3,4] Since the International Agency for Research on Cancer (IARC) designated *H. pylori* as a group 1 carcinogen, its infection is regarded as a leading risk factor for gastric cancer.[5,6] A key contributor to its pathogenicity is its highly active urease production, which enables its long-term colonization in the acidic environment of the stomach.

Urease (EC 3.5.1.5) is a nickel-dependent enzyme broadly distributed in bacteria, fungi, algae, and plants.[7,8] Its catalytic activity relies on nickel ions and a carbamylated lysine residue at the active site.[9,10] Excessive urease activity leads to the overproduction of ammonia and elevated pH levels, resulting in detrimental impacts on agriculture, ecosystems, and human health.[11] In agriculture, elevated urease activity drives substantial ammonia volatilization during urea fertilization, leading to environmental pollution and economic loss.[12] In humans, bacterial urease promotes the progression of various diseases; for example, urease from urinary tract pathogens such as the

[a]*Department of Pharmaceutical Sciences, Zunyi Medical University, Zhuhai Campus, Zhuhai, 519041, China. E-mail: luqiang@zmu.edu.cn; Tel: +86 756 762 3384*

[b]*Department of Pharmacology, Zunyi Medical University, Zhuhai Campus, Zhuhai, 519041, China. E-mail: licailan@zmu.edu.cn; Tel: +86 756 762 3384*

[c]*Key Laboratory of Basic Pharmacology of Ministry of Education and Joint International Research Laboratory of Ethnomedicine of Ministry of Education, Zunyi Medical University, Zunyi, 563000, China*

[d]*Key Laboratory of Basic Pharmacology of Guizhou Province and School of Pharmacy, Zunyi Medical University, Zunyi, 563000, China*

Proteus species alkalizes urine and contributes to crystal precipitation and stone formation.[13] For *H. pylori*, the urease-mediated hydrolysis of urea generates ammonia and carbon dioxide, establishing a localized neutral microenvironment that facilitates its survival and colonization and the development of chronic gastric inflammation.[14] Although antibiotics can treat *H. pylori* infection, the increasing prevalence of antibiotic resistance highlights the urgent need for alternative therapeutic strategies, including the development of novel urease inhibitors.

The existing urease inhibitors are generally classified into substrate analogues (*e.g.*, hydroxamic acids[15] and phosphate esters[16]) and non-substrate analogues (*e.g.*, imidazole derivatives,[17] polyphenols,[18] and metal complexes).[19] Although phosphate esters show strong inhibitory potency, they are unstable under acidic gastric conditions, limiting clinical use.[20] Hydroxamic acids typically exhibit favorable aqueous solubility. However, their clinical application as urease inhibitors can be significantly limited by severe adverse effects, such as teratogenicity.[21] These limitations highlight the need for safe, naturally derived urease inhibitors.

Oleuropein ($C_{25}H_{32}O_{13}$, Fig. 2A), the predominant secoiridoid phenolic compound found in the olive tree (*Olea europaea* L), occurs especially in fresh olive fruits and leaves.[22,23] This key bioactive constituent of olive products has attracted wide scientific attention due to its varied beneficial effects on health, including potent antioxidant,[24] anti-inflammatory,[25] antimicrobial,[26] and gastric protective activities.[27] The molecular structure of oleuropein, characterized by an *ortho*-diphenolic group, not only confers a powerful radical-scavenging capacity but also enables it to modulate various cellular signaling pathways. Recent evidence has further illuminated the inhibitory effects of olive leaf extracts and oleuropein against *H. pylori* infections.[28–30] However, its precise molecular targets and the underlying mechanisms remain poorly defined. In particular, whether oleuropein directly targets the urease system, a key virulence factor required for *H. pylori* survival in the acidic gastric environment, has not been systematically investigated.

Based on network pharmacology predictions, this study aimed to systematically assess the inhibitory effect of oleuropein on the crude *H. pylori* urease extract (HPU) and elucidate the underlying mechanism. Using jack bean urease (JBU) as a reference enzyme, we conducted enzyme inhibition assays, kinetic studies, inhibition-site analysis, reactivation experiments, and molecular docking. To the best of our knowledge, this is the first study to integrate network pharmacology with enzymatic and mechanistic analyses to investigate oleuropein targeting HPU. These investigations provide insights into the anti-*H. pylori* activity of oleuropein and support its potential as a naturally derived urease-targeting lead compound.

2. Materials and methods

2.1 Chemicals and reagents

Oleuropein ($C_{25}H_{32}O_{13}$, CAS: 32619-42-4, purity ≥98%) was obtained from Chengdu Desite Biotechnology Co., Ltd JBU (type III, 40.3 units per mg solid) and urea were purchased from Sigma Aldrich (St. Louis, USA). Acetohydroxamic acid (AHA), boric acid (BA), sodium fluoride (NaF), sodium nitroprusside, sodium salicylate, and sodium hypochlorite were procured from Shanghai McLean Biochemical Technology Co., Ltd. Dithiothreitol (DTT) and L-cysteine (L-cys) were acquired from Beijing Solarbio Science & Technology Co., Ltd., while glutathione (GSH) was obtained from Dalian Meilun Biotechnology Co., Ltd. Sodium hydroxide (NaOH) was sourced from Tianjin Damao Chemical Reagent Factory. All reagents used in this study were of analytical-grade purity.

2.2 Network pharmacology

2.2.1 Data source and preparation. The canonical SMILES of oleuropein was retrieved from the PubChem database to define its chemical structure for the study. Concurrently, a proteome-wide set of protein sequences for *H. pylori* was obtained by searching and downloading all reviewed entries from the UniProt database, yielding 613 reviewed protein sequences for subsequent computational screening.

2.2.2 Prediction of potential drug-target interactions. The binding affinities between oleuropein and the *H. pylori* proteome were predicted using the DeepPurpose computational framework. The pre-trained model "model_mpnn_aac_davis" was employed for this large-scale virtual screening to identify potential protein targets with high binding potential.

2.2.3 Construction and analysis of the protein–protein interaction (PPI) network. Potential target proteins identified from the DeepPurpose prediction were used to construct a PPI network using the STRING database. The resulting network was imported into Cytoscape software (version 3.10.1) for visualization and further topological analysis. To identify highly interconnected functional clusters, the MCODE plugin was applied to the PPI network. The proteins within the top-scoring modules were considered key functional targets for subsequent analysis.

2.3 *H. pylori* culture and preparation of crude *H. pylori* urease extract

H. pylori was cultivated on Columbia agar supplemented with bovine serum albumin under microaerophilic conditions (5% O_2, 10% CO_2 and 85% N_2) at 37 °C for 72 hours. The method for HPU extraction was adapted from a study by Xiao *et al.*[31] Fifty milliliters of *H. pylori* solution was centrifuged (5000 rpm, 4 °C, 10 minutes) to obtain precipitated bacteria, which were washed twice with PBS, and the suspensions were stored at −80 °C for 24 hours. Primarily, the frozen bacterial solution was thawed and allowed to equilibrate at room temperature. Subsequently, three milliliters of distilled water and protease inhibitor were added to the bacterial solution, mixed, sonicated for 1 min, centrifuged (15 000 rpm, 4 °C, 10 minutes) and desalted. Ultimately, the supernatant was collected as the crude *H. pylori* urease (HPU) extract, and the obtained extract was mixed with the same volume of glycerol and stored at 4 °C.

2.4 Standard urease activity test

The standard urease test mixture consists of 150 mM urea and a 20 mM HEPES buffer (pH = 7.5), and the reaction is initiated

upon the addition of different concentrations of urease solutions. After 20 minutes of continuous reaction at room temperature, the ammonia produced was determined at 595 nm through an improved phenol-hypochlorite method to evaluate urease activity.[32] Under these conditions, the specific activity of HPU was 17.0 U mg^{-1}, compared with 40.3 U mg^{-1} for JBU.

2.5 Urease inhibition experiment

To assess inhibition, urease was pre-incubated with various concentrations of oleuropein or AHA in the 20 mM HEPES buffer (pH = 7.5) for 20 min at 37 °C. The reaction was then initiated by adding 150 mM urea, and the ammonia produced was quantified at 595 nm using the Berthelot reagent. The urease activity in the absence of an inhibitor was used as the control and defined as 100% activity. Residual activity (RA%) was calculated as the percentage of activity relative to this uninhibited control. The IC_{50} value, representing the inhibitor concentration that reduced activity by 50%, was subsequently determined. Results are expressed as the mean of three independent replicates.

2.6 Inhibition kinetic study

The inhibition mode of oleuropein against urease was investigated using Lineweaver–Burk plots, where the reciprocal of reaction velocity was plotted against the reciprocal of substrate concentration. The kinetic parameters, Michaelis constant (K_M) and the maximum velocity (v_{max}), were derived in the presence of varying oleuropein concentrations to characterize the inhibition type. Furthermore, secondary plots were constructed by plotting oleuropein concentration against the slope or intercept to determine the inhibition constants K_i and K_{is}.

2.7 Analysis of reaction progress curve

The time-dependent inhibition of urease by oleuropein was examined by monitoring ammonia formation over time. Two experimental setups were compared: a direct assay and a pre-incubation assay. In the direct assay, the reaction was triggered by mixing a solution containing urease and varying concentrations of oleuropein with the urea substrate. In the pre-incubation assay, urease was first incubated with oleuropein for 20 minutes at 37 °C prior to the addition of urea to start the reaction. Urease activity at designated time points was determined using a standard method, and the resulting data were fitted to a curve for analysis.

2.8 Urease protection test

To probe the molecular target of oleuropein inhibition, HPU was pre-incubated with protective compounds known to bind specifically to the active site. These included sulfhydryl agents (DTT, L-cys, GSH) that engage the critical thiol group and inorganic agents (BA, NaF) that coordinate the catalytic Ni^{2+}. This pre-incubation (20 mM HEPES, pH = 7.5, 37 °C, 20 minutes) was followed by the addition of oleuropein and a further 20-minute incubation. The residual urease activity was then determined in triplicate.

2.9 Oleuropein-sulfhydryl interaction test

The protective effects of sulfhydryl compounds (DTT, L-cys, and GSH) on the inhibition of the enzyme by oleuropein were investigated at varying incubation times and with different addition sequences. In short, the sulfhydryl compound, oleuropein and HPU in the mixture were incubated at 37 °C for 5, 10, 30, and 40 minutes. In the interaction-sequence experiment involving oleuropein, sulfhydryl compounds, and urease, any two of the three components were first pre-incubated at 37 °C for 20 minutes. The third component was then added, and the resulting mixture was further incubated at 37 °C for an additional 20 minutes.

2.10 Reactivation of oleuropein-inactivated urease

The restoration of enzyme activity suppressed by oleuropein was examined in the presence of protective agents. First, the enzyme was inactivated by pre-incubation with oleuropein in the 20 mM HEPES buffer (pH = 7.5) at 37 °C for 20 minutes. Then, 1.25 mM of a protective agent was added to the mixture. Finally, the residual enzyme activity was measured at different incubation times to monitor the extent of reactivation.

2.11 Molecular docking

The molecular docking of oleuropein with urease was carried out using AutoDock Vina. The three-dimensional crystal structures of both HPU (PDB ID: 1E9Z) and JBU (PDB ID: 4GOA) were obtained from the Protein Data Bank (PDB) and prepared by removing all crystallographic water molecules and non-essential heteroatoms, followed by the addition of polar hydrogens using AutoDockTools. The 3D structure of oleuropein was obtained from PubChem and then converted into the required PDBQT format. The docking grid box was centered on the active site region of each urease. Default Autodock Vina parameters were used, and the highest-scoring conformations from Autodock Vina were analyzed and visualized using PyMOL.

2.12 Statistical analysis

Data from three independent experiments were plotted using GraphPad Prism 8.0, and the results were represented as the means ± standard errors. Data differences were analyzed using one-way ANOVA with Dunnett's post–hoc test in SPSS 29.0. A P value below 0.05 was considered statistically significant.

3. Results

3.1 Target prediction and protein–protein interaction network analysis of oleuropein against *H. pylori*

To elucidate the mechanisms of oleuropein against *H. pylori*, a target prediction was performed using the DeepPurpose computational framework. As shown in Fig. 1, a total of 72 *H. pylori* proteins were identified as potential targets of oleuropein with a predicted binding affinity threshold of $-\log(K_d) > 10$, suggesting potential binding interactions.

Subsequently, a PPI network was constructed with these potential targets to explore their functional relationships. After

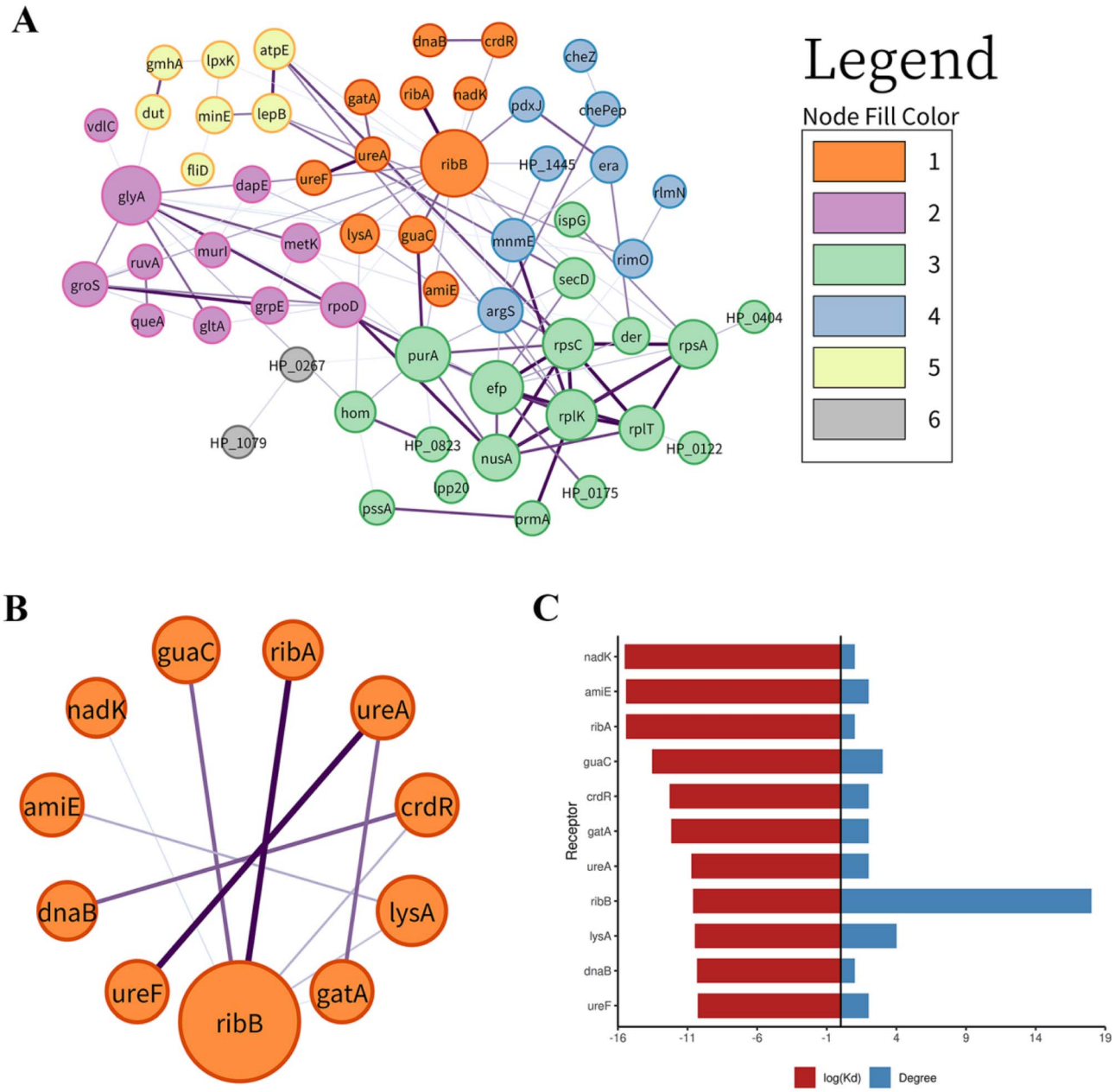

Fig. 1 Network pharmacology analysis of oleuropein targets against *H. pylori*. (A) Protein–protein interaction (PPI) network of oleuropein-associated *H. pylori* target proteins. (B) Subnetwork of Module 1 target proteins. (C) Bar chart showing the predicted dissociation constants ($-\log(K_d)$) of oleuropein binding and the corresponding degree values for Module 1 targets.

filtering, a robust PPI network comprising 58 nodes was established. A module analysis of this network revealed several topological modules. Notably, Module 1 was identified as the most significant functional cluster, as it housed the hub node with the highest degree value in the entire network. Critically, this module encompassed key components of the urease complex (UreA and UreF), a virulence factor essential for *H. pylori* colonization and survival in the acidic gastric environment. The enrichment of targets involved in central metabolism alongside urease subunits within Module 1 strongly suggests a synergistic multi-target action of oleuropein. This computational evidence positioned the urease system as a high-priority target for the subsequent experimental validation of its inhibition.

3.2 Inhibitory effects of oleuropein on urease

Guided by the network pharmacology prediction that positioned the urease complex as a high-priority target, we experimentally assessed the inhibitory effect of oleuropein on HPU. To better interpret the biological relevance of this effect, JBU was also tested as a non-bacterial reference urease. This

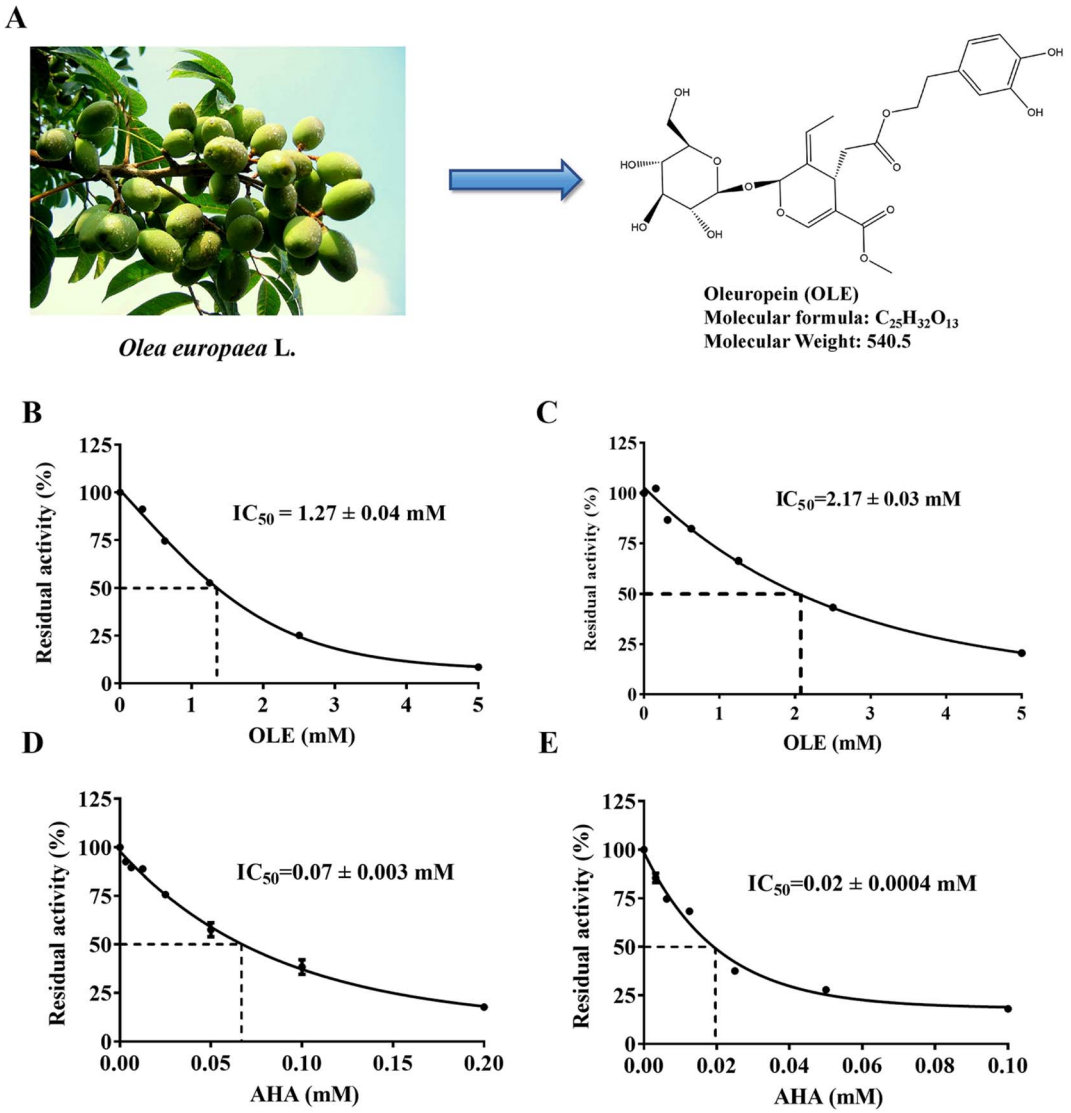

Fig. 2 Suppressive effect of oleuropein (OLE) towards HPU and JBU activity. (A) Plant source and chemical structure of OLE. The enzyme was treated with OLE (B for HPU and C for JBU) and AHA (D for HPU and E for JBU). Each experiment was conducted in triplicate.

comparison allowed us to determine whether oleuropein acted as a general urease inhibitor or exhibited differential inhibition toward the bacterial enzyme.

The results demonstrated that oleuropein significantly inhibited the activity of both ureases in a dose-dependent manner (Fig. 2B and C). The calculated IC_{50} values for oleuropein were 1.27 ± 0.04 mM for HPU and 2.17 ± 0.03 mM for JBU, confirming its broad, yet more potent, functional impact on the bacterial enzyme. For comparison, the well-characterized urease inhibitor AHA (Fig. 2D and E), used as a positive control, exhibited IC_{50} values of 0.07 ± 0.003 mM for HPU and 0.02 ± 0.0004 mM for JBU under the same experimental conditions.

The successful experimental validation of the urease inhibition functionally corroborates our initial computational prediction. The observed potency against HPU highlights oleuropein's potential to specifically target a critical virulence factor in *H. pylori*.

3.3 Determination of K_M and V_{max}

The Michaelis constant (K_M) and maximum velocity (V_{max}) were determined using Lineweaver–Burk plots to investigate the inhibition type and mechanism of oleuropein on urease. As shown in Fig. 3A, the lines intersect at a defined point in the second quadrant. The K_M gradually increased, and V_{max} progressively decreased with an increase in the concentrations of the inhibitor, revealing that oleuropein is a mixed-type inhibitor for HPU. In addition, the values of the equilibrium inhibitory constants for the binding of oleuropein to the free enzyme K_i and the enzyme-substrate complex K_{is} were 0.58 ± 0.02 and 0.69 ± 0.01 mM, respectively, which were calculated from the replots of inhibitor concentration *versus* slope or intercept (Fig. 3B and C).

For JBU, the lines intersect at a specific point on the *x*-axis (Fig. 3D). The K_M remained relatively stable, while V_{max} gradually decreased with an increase in inhibitor concentration,

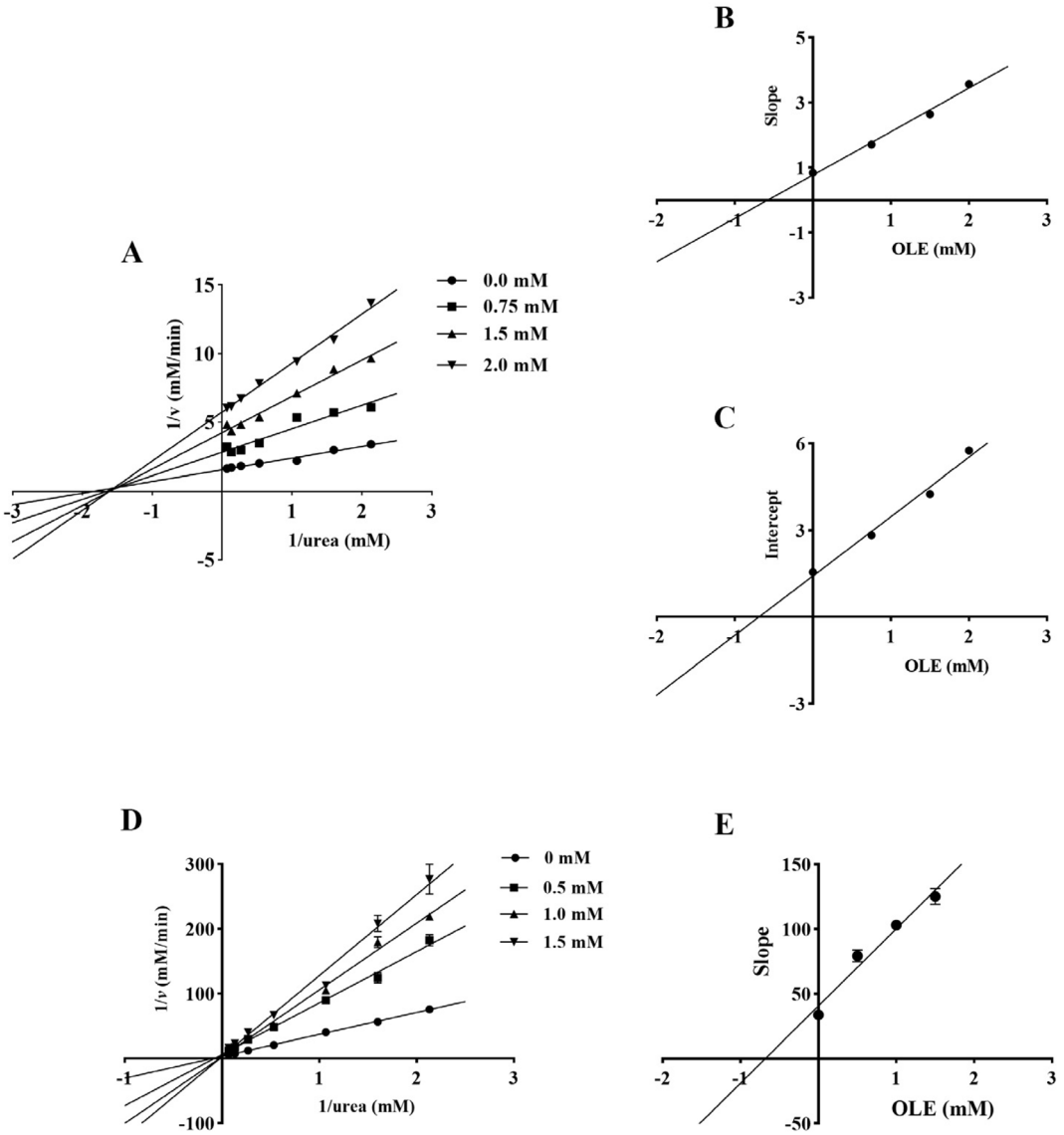

Fig. 3 Kinetic analyses of urease suppression by oleuropein (OLE). (A) Lineweaver–Burk plots for HPU in the absence and presence of different concentrations of OLE. (B and C) Secondary plots of slope and intercept *versus* OLE concentration for HPU used to determine the inhibition constants K_i and K_{is}. (D) Lineweaver–Burk plots for JBU in the absence and presence of different concentrations of OLE. (E) Secondary plot of slope *versus* OLE concentration for JBU used to determine the inhibition constant K_i. Each experiment was conducted in triplicate.

which is characteristic of non-competitive inhibition. The value of the equilibrium inhibitory constant K_i was determined to be 0.69 ± 0.04 mM (Fig. 3E).

3.4 Reaction progress curve

The reaction progress curves for urease inhibition by oleuropein revealed a distinct time-dependent behavior, as shown in Fig. 4. A critical difference was observed between the non-preincubated and preincubated systems.

In the non-preincubated system (Fig. 4A and C), where the enzyme, substrate, and inhibitor were mixed simultaneously, the reaction progress curves showed a linear trend. This indicates that the full inhibitory effect was not immediate, and the enzyme maintained a relatively constant rate of substrate hydrolysis throughout the assay period.

In contrast, the preincubated system (Fig. 4B and D), where the enzyme was pre-mixed with the inhibitor before the reaction was initiated by adding the substrate, exhibited concave-downward curves. This shape is characteristic of a process where the inhibitor's effect develops over time. The pre-incubation period allowed oleuropein to bind to the enzyme, forming an initial complex. Upon substrate addition, this complex undergoes a time-dependent transition to a more stable, fully inhibitory complex (EI*), resulting in a progressive decrease in reaction velocity from an initial rate (V_0) to a final steady-state rate (V_s). This clear contrast confirms that the inhibition of urease by oleuropein is time-dependent, which is consistent with a slow-binding inhibition mechanism.[33,34]

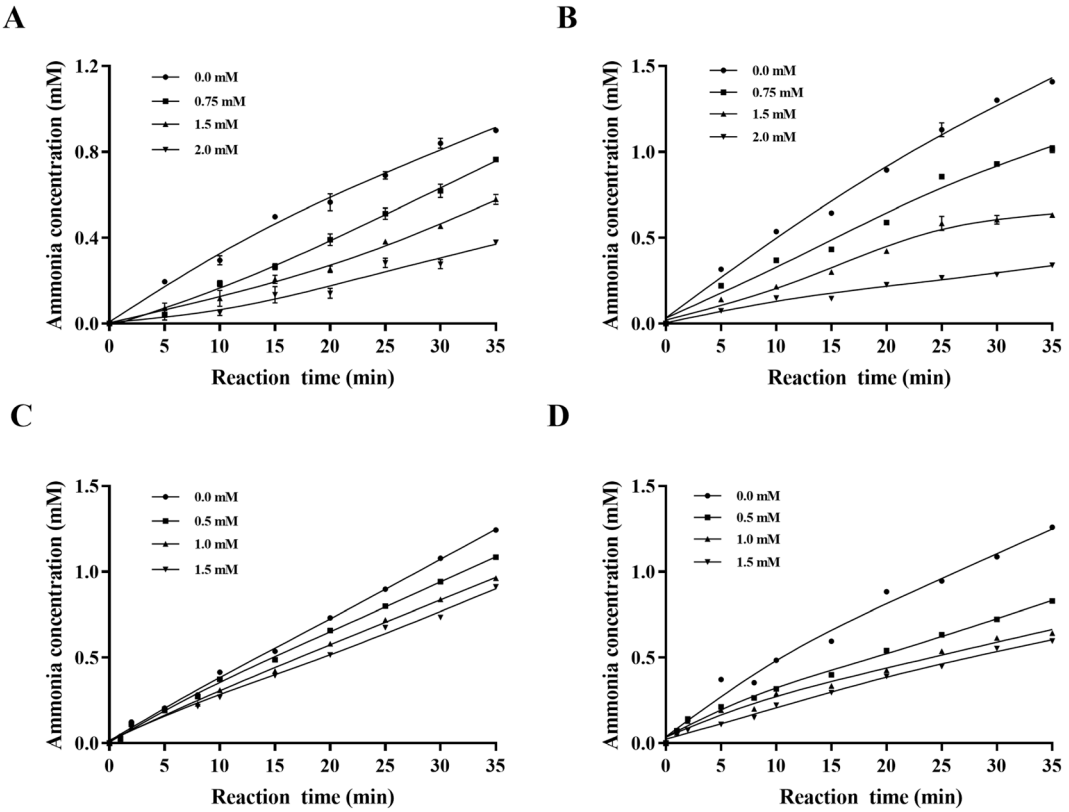

Fig. 4 Reaction progress curves for urease-catalyzed urea hydrolysis in the absence and presence of oleuropein (OLE). (A and B) Progress curves for HPU under non-preincubated and preincubated conditions. (C and D) Progress curves for JBU under non-preincubated and preincubated conditions. In the preincubated system, urease was incubated with OLE before the addition of urea. Ammonia production was monitored over time. Each experiment was repeated three times.

3.5 Protective test of the oleuropein-inhibition urease

This study investigated the potential interaction sites of oleuropein on urease by using sulfhydryl compounds (DTT, GSH, and L-cys) and inorganic compounds (BA and NaF). Fig. 5A and B showed that the residual urease activity of oleuropein-inhibited urease in the thiol-containing compound system was higher than that in the thiol-free system. Sulfhydryl compounds markedly diminished oleuropein-induced urease inactivation, indicating that oleuropein might interact with the sulfhydryl site of urease. In addition, Fig. 5C and D demonstrated that the residual urease activity in the inorganic compound system, which included oleuropein, BA, NaF, and urease, was significantly lower than that in the system with oleuropein without the presence of inorganic compounds. In conclusion, the protective effect of sulfhydryl compounds is greater than that of inorganic compounds, suggesting that sulfhydryl groups at or near the urease active site may be involved in oleuropein-mediated inhibition.

3.6 Oleuropein-thiol-urease interaction test

As shown in Fig. 6, the inhibitory effect of oleuropein on urease intensified with a prolonged incubation time. However, the protective action of thiols (DTT, GSH, L-cys) against this inhibition was not time-dependent (Fig. 6A and B). Moreover, urease activity varied according to the sequence in which oleuropein, urease, and thiols were added. Higher activity was observed when thiol reagents were introduced before oleuropein, compared with their addition after oleuropein had already interacted with urease (Fig. 6C and D). Overall, these findings highlight the essential role of thiol groups in the oleuropein-induced inactivation of HPU and JBU.

3.7 Reactivation of oleuropein-inactivated urease

As illustrated in Fig. 7, following its reaction with oleuropein, urease suffered an activity loss of approximately 80%. After adding 1.25 mM DTT, the activity of the oleuropein-inhibited HPU and JBU recovered in a time-dependent pattern, with maximum reactivation reaching approximately 40% and 30% of the original activity, respectively, indicating that the inactivation was reversible. It was further verified that the recovery of the activity of the oleuropein-inactivated urease by sulfhydryl compounds was consistent with the protection test results, suggesting that the interaction between oleuropein and the sulfhydryl group at the active site of urease is crucial for the inhibition.

3.8 Molecular docking analysis

To explore a possible structural basis for the inhibition, we performed the molecular docking of oleuropein into the

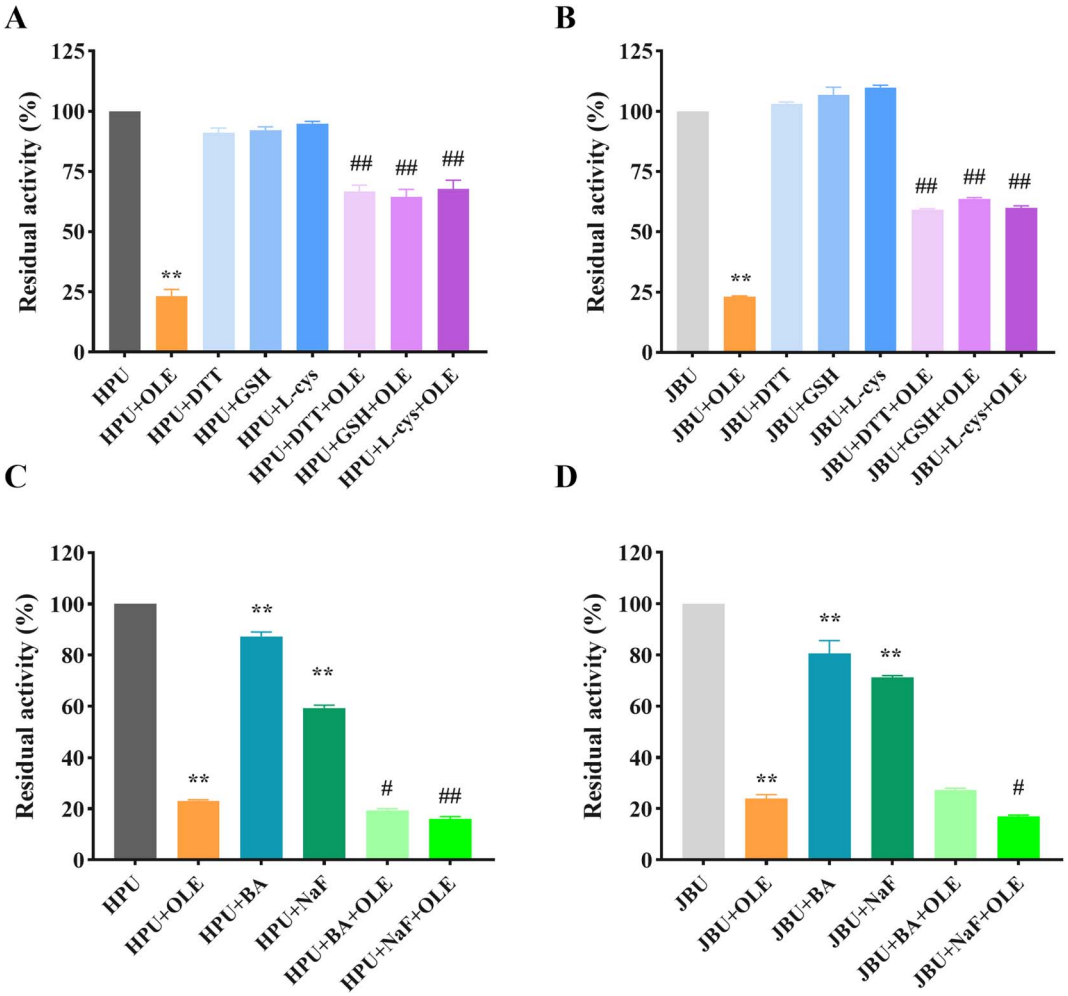

Fig. 5 Protective roles of thiol-containing compounds and inorganic agents against urease inhibition by oleuropein (OLE). Panels A and B depict the effects of thiol reagents (DTT, GSH, L-cys) on the OLE-induced loss of HPU and JBU activities. Panels C and D present the influence of inorganic substances (BA, NaF) on the OLE-mediated suppression of HPU and JBU activities. OLE was used at concentrations of 2.5 mM (for HPU) and 4.5 mM (for JBU). Data are reported as the mean ± SEM of three independent assays. $^{**}P < 0.01$ *vs.* the urease group; $^{\#}P < 0.05$, $^{\#\#}P < 0.01$ *vs.* the OLE group.

catalytic core of the HPU and JBU. As depicted in Fig. 8, the results suggest a potential pattern of oleuropein and urease binding. In this research, the binding free energy values from HPU and JBU were −5.451 and −5.026 kcal mol^{-1}, respectively. The optimal binding modes of oleuropein are represented in the enzyme surface (Fig. 8A and C) and cartoon mode (Fig. 8B and D), respectively. For HPU, oleuropein primarily interacts with residues in the flap region, including CYS321, MET319, HIS323, GLN364, MET366, and GLY367, through hydrogen bonding. This region is located on the mobile flap that closes the active site. Moreover, the amino acid residues, ASN168, VAL320, and ARG368, formed hydrophobic interactions with oleuropein.

For JBU, oleuropein formed hydrogen bonds with ALA436, ARG439, ALA440, HIS492, ASP494, GLY550, ASP633, GLN635 and ALA636, respectively. The benzene ring of oleuropein established hydrophobic bonds with protein residues CYS592, LYS490, HIS519, VAL591, HIS593, and HIS594. These results further support the possibility that sulfhydryl-containing residues at or near the active site are involved in the overall process of oleuropein-mediated urease. This finding aligns with the outcomes observed in both the protection and reactivation tests, thereby supporting a possible mechanism for oleuropein-mediated urease inhibition.

4. Discussion

Persistent colonization by *H. pylori* is a major risk factor for chronic gastritis, peptic ulcer disease, and gastric cancer. Among its virulence factors, urease plays a central role in enabling bacterial survival in the highly acidic gastric environment by generating ammonia and creating a locally neutral microenvironment. Therefore, urease has long been regarded as a strategic target for controlling *H. pylori* infection.[35,36] In this study, we combined network pharmacology, enzymatic characterization, and molecular docking to systematically investigate

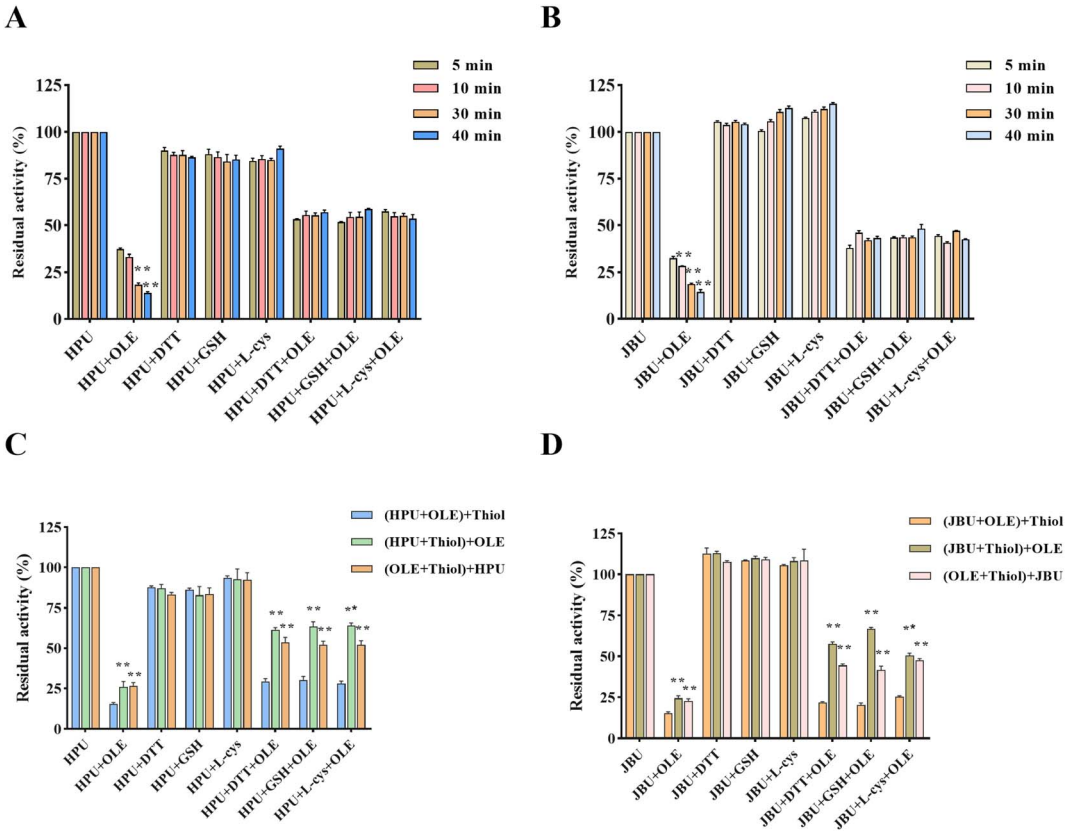

Fig. 6 Protective role of incubation duration and the order of introducing thiol compounds toward oleuropein (OLE)-modified HPU (A and C) and JBU (B and D). Enzymatic activity was measured after coincubation for 5, 10, 30, or 40 minutes. For conditions in which components were grouped in brackets, those elements were pre-incubated for 20 minutes before adding the remaining components for an additional 20-minute coincubation. In all experiments, OLE was used at 2.5 mM (HPU) or 4.5 mM (JBU). Data represent the mean ± SEM from three independent experiments. $^{**}P < 0.01$ *versus* the first column of each group.

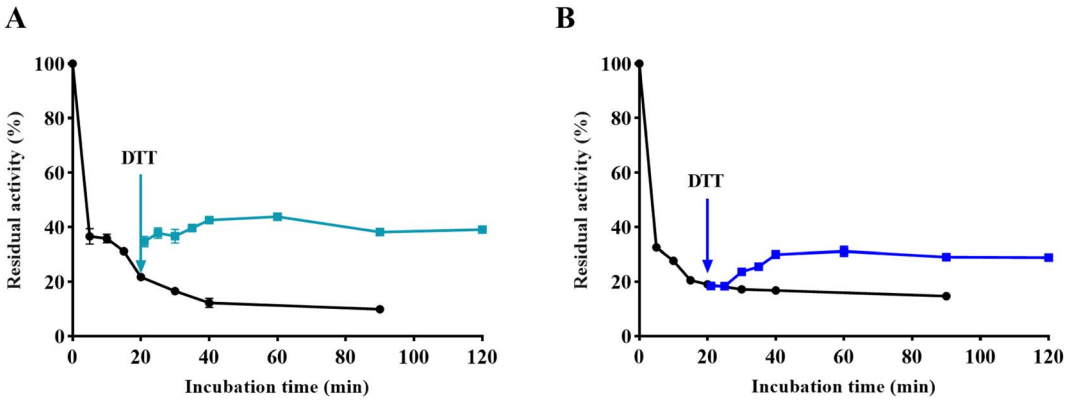

Fig. 7 Enzymatic reactivation of oleuropein (OLE)-evoked suppression of HPU (A) and JBU (B) by DTT. The activity of urease was restrained by OLE (●) (2.5 mM for HPU and 4.5 mM for JBU) and subsequently assessed following the addition of 1.25 mM DTT (■). The test was performed in triplicate.

the interaction between oleuropein, a natural secoiridoid from olive leaves, and urease from *H. pylori*.

Our network-based analysis predicted 72 putative *H. pylori* protein targets of oleuropein. Within the constructed PPI network, urease-related proteins, specifically UreA and UreF, clustered within a highly connected functional module alongside proteins involved in central metabolism. UreA is a structural subunit essential for the formation of the urease active site,[37] while UreF functions as a nickel chaperone critical for nickel insertion and enzyme maturation.[38] Their topological prominence and co-localization in this functional module suggest that the urease system may represent a critical point of

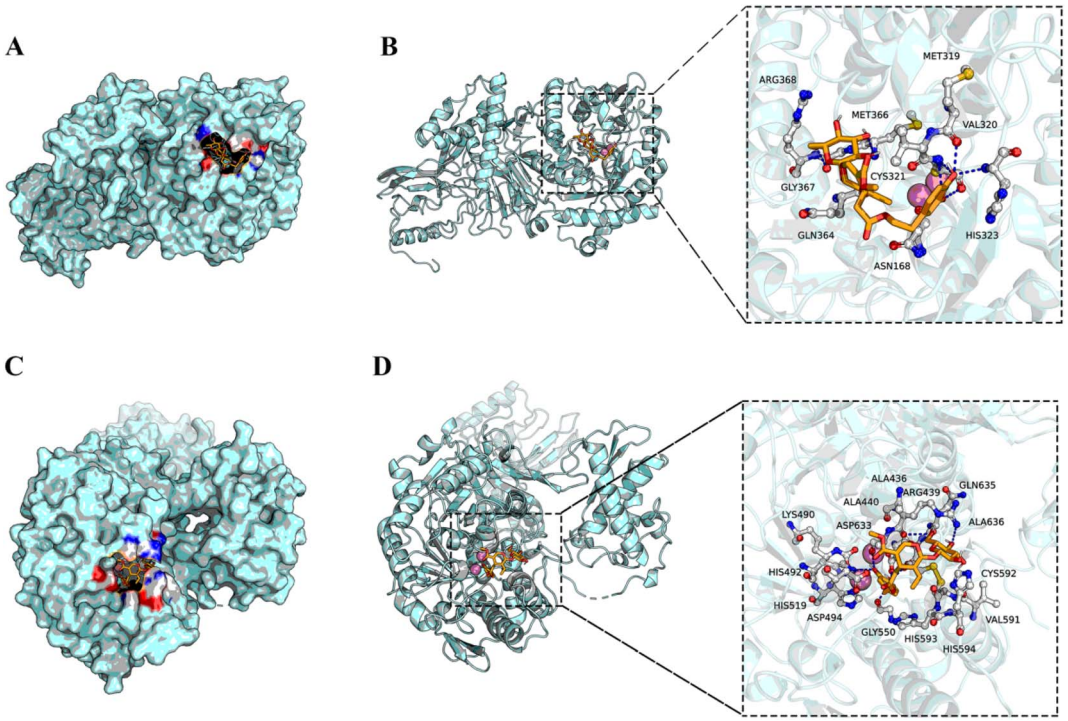

Fig. 8 Molecular docking analysis was conducted to examine the interactions between oleuropein and HPU (A and B), as well as JBU (C and D). The surface and cartoon representations illustrate these interactions. The blue dashed lines indicate hydrogen bonds.

intervention for oleuropein's anti-*H. pylori* action. Based on this prediction, we selected urease as a key target for experimental validation and mechanistic investigation.

Enzymatic assays confirmed that oleuropein inhibits both HPU and JBU in a concentration-dependent manner, with somewhat higher potency against HPU. The calculated IC_{50} for HPU (1.27 ± 0.04 mM) was lower than that for JBU (2.17 ± 0.03 mM), indicating a potentially greater affinity for the bacterial enzyme. The inclusion of JBU as a reference urease is important because it helps distinguish general urease inhibition from inhibition that may be more relevant to the bacterial enzyme. Although oleuropein inhibited both enzymes, its relatively stronger effect on HPU suggests potential biological relevance to its anti-*H. pylori* activity. Although the IC_{50} values of oleuropein are in the millimolar range and, therefore, indicate lower potency than that of the classical urease inhibitor AHA, they are within the typical range for many unoptimized natural products.[39,40] Together with the favorable safety profile of oleuropein as a dietary component, these findings support its potential as a lead compound or adjunctive agent rather than a direct replacement for existing urease inhibitors.

From a translational perspective, oleuropein may represent a promising scaffold for further development. Future studies are warranted to optimize its structure for improved potency and selectivity and to validate its activity in cell-based *H. pylori* infection models and *in vivo* infection models. In addition, its natural origin and favorable safety profile suggest potential utility as an adjunctive agent in anti-*H. pylori* therapy.

Detailed kinetic analysis revealed important differences in the inhibition modes of oleuropein toward ureases from different sources. For HPU, Lineweaver–Burk plots indicated a mixed-type inhibition pattern, characterized by an increase in K_M and a decrease in V_{max} with increasing oleuropein concentrations. This suggests that oleuropein can bind both the free enzyme and enzyme-substrate complex, at a site that partially overlaps with or is allosterically coupled to the substrate-binding region. In contrast, the inhibition of JBU was consistent with a noncompetitive mechanism, manifesting as a reduced V_{max} with minimal change in K_M. The observed divergence in inhibition patterns is likely rooted in distinct structural features between HPU and JBU. JBU, the first urease extracted from plants, has been widely used as a model enzyme.[41,42] Structurally, JBU is composed of six identical subunits, totaling 90 cysteine residues, with each monomer containing two nickel ions and fifteen cysteine residues.[43,44] In contrast, HPU is a heterooligomer composed of α and β subunits, which distinguishes it from the monomeric structures of ureases of fungi, bacteria, and plants.[45]

The reaction progress curves further demonstrated that oleuropein is a slow-binding inhibitor of both HPU and JBU. In assays without pre-incubation, the reaction proceeded approximately linearly, suggesting that the full inhibitory effect developed over time. In contrast, the pre-incubation of urease with oleuropein before substrate addition produced concave-downward progress curves, indicative of a time-dependent decrease in reaction rate. This kinetic behavior is consistent with a two-step inhibition mechanism, in which an initial EI complex forms rapidly and then slowly converts into a more tightly bound EI* complex. Such slow-binding characteristics are often associated with conformational rearrangements of the

enzyme or the inhibitor and are considered advantageous from a pharmacological standpoint because they can prolong the target residence time *in vivo*.

Protection and reactivation experiments with thiol-containing reagents provided additional mechanistic insight. Specifically, the sulfhydryl compounds like DTT, GSH, L-cys react with the thiol groups,[46] while the inorganic reagents, such as BA and NaF, interact with the nickel ions located in the urease active center.[47] In the present study, DTT, GSH, and L-cys markedly attenuated the inhibitory effect of oleuropein on urease and promoted the recovery of activity in oleuropein-treated enzymes, whereas inorganic agents that target the nickel center (BA, NaF) afforded weaker protection. These observations strongly implicate sulfhydryl groups, most likely cysteine residues, as key sites for oleuropein interaction. The fact that inhibition is reversible and can be reversed by thiol reagents argues against irreversible covalent modification or non-specific denaturation and, instead, suggests a reversible, thiol-sensitive interaction at or near the active site.

Molecular docking provided a plausible structural basis for the observed inhibition. The simulations suggested that oleuropein stably binds within the active site pocket of HPU, and its binding site directly encompasses the key cysteine residue CYS321 in the flap region. This residue engages in strong hydrophobic interactions with oleuropein. Similarly, interaction with the corresponding cysteine residue (CYS592) in JBU was observed. Although CYS321 is not directly involved in nickel ion coordination in urease, its location in the flap region is crucial for maintaining the correct active site conformation and the open-close movement of the flap.[48,49] By binding to CYS321 and other residues, oleuropein likely "locks" the flap, hindering its necessary conformational changes, thereby impeding substrate access or product release. This is consistent with the observed mixed-type inhibition and time-dependent characteristics.

Our findings are in line with previous reports that various natural polyphenols and plant-derived compounds inhibit urease, typically by interacting with active-site residues. Consistent with this, several phytochemicals, including baicalin ($IC_{50} = 0.82 \pm 0.07$ mM), scutellarin ($IC_{50} = 0.47 \pm 0.04$ mM),[50] piceatannol ($IC_{50} = 0.67 \pm 0.02$ mM),[51] patchouli alcohol ($IC_{50} = 2.67 \pm 0.79$ mM),[52] and andrographolide ($IC_{50} = 3.175 \pm 0.34$ mM)[53] have been reported to inhibit HPU by targeting urease sulfhydryl groups. Notably, oleuropein exhibits urease inhibitory potency within a similar order of magnitude, being less potent than scutellarin, baicalin, and piceatannol but comparable to or greater than patchouli alcohol and andrographolide. More importantly, oleuropein exhibits a distinctive combination of features, including a slight preference for bacterial over plant urease and a slow-binding, mixed-type inhibition of HPU. These characteristics, together with its favorable safety profile as a dietary component, make oleuropein an attractive and complementary scaffold to existing thiol-dependent natural urease inhibitors for further structural optimization aimed at improving its potency and selectivity toward HPU.

Despite these advances, several limitations of this study should be acknowledged. First, all mechanistic experiments were carried out *in vitro*, and the anti-*H. pylori* efficacy of oleuropein was not evaluated in cellular or *in vivo* infection models. Second, although the crude *H. pylori* urease extract (HPU) used in this study showed measurable urease activity, it may still contain non-urease proteins that could potentially interact with sulfhydryl compounds, protective agents, or inorganic reagents, thereby influencing the results of the protection, sulfhydryl interaction, and reactivation assays to some extent. Nevertheless, the overall consistency observed across multiple independent approaches, including inhibition kinetics, protection and reactivation experiments, and molecular docking analysis, strongly supports urease as a primary target of oleuropein. In addition, the use of JBU as a reference enzyme provides support for the proposed inhibitory mechanism. Third, although our network pharmacology analysis suggested multiple potential targets of oleuropein in *H. pylori*, this study focused exclusively on urease, and other predicted targets remain to be validated. Addressing these limitations will require future studies using purified urease or recombinant enzyme systems, together with site-directed mutagenesis of key residues, such as CYS321, validation in cell-based *H. pylori* infection systems, and the *in vivo* evaluation of oleuropein or its derivatives in infection models.

5. Conclusion

This study demonstrated that oleuropein effectively inhibited the activity of the crude *H. pylori* urease (HPU) extract in a time-dependent manner and exhibited a mixed-type inhibition pattern. Mechanistic analyses suggest that this inhibitory effect is associated with interaction with sulfhydryl groups at or near the urease active site, particularly involving the flap-region residue CYS321. These findings provide mechanistic insights into the anti-*H. pylori* activity of oleuropein and support its potential as a natural lead compound for urease-targeted intervention.

Author contributions

Conceptualization and supervision: Q. L. and C. L.; methodology and investigation: L. Z., H. C., D. Z., J. W. and L. T.; writing – original draft: L. Z.; formal analysis and visualization: H. C., D. Z. and J. W.; resources: Q. L. and C. L.; and writing – review and editing: Q. L. and C. L. All authors have read and agreed to the published version of the manuscript.

Conflicts of interest

The authors declare no conflict of interest.

Data availability

The datasets generated for this study are available upon request to the corresponding authors.

Acknowledgements

This study was supported by the National Natural Science Foundation of China (No. 82360809 and 82304828), the Future "Science and Technology Elite" Project (No. ZYSE-2022-01 and ZYSE-2025-04), and the Key Project of the Department of Education of Guangdong Province (No. 2023ZDZX2076).

References

1 J. Li, S. S. Liu, Z. Q. Li, C. L. Ma, B. Q. Li, Y. Z. Cui, W. K. Wang, H. L. Zhao, X. F. Ji and Y. Zhang, Autophagy-driven modulation of stem cell dynamics in Helicobacter pylori-induced gastric diseases in mice, *Virulence*, 2025, **16**, 2551176.

2 X. B. Xu, X. Fei, H. Wang, X. D. Wu, Y. Zhan, X. Li, Y. A. Zhou, C. X. Shu, C. He, Y. Hu, J. P. Liu, N. Lv, N. H. Li and Y. Zhu, *Helicobacter pylori* infection induces DNA double-strand breaks through the ACVR1/IRF3/POLD1 signaling axis to drive gastric tumorigenesis, *Gut Microbes*, 2025, **17**, 2463581.

3 L. Xie, G. W. Liu, Y. N. Liu, P. Y. Li, X. N. Hu, X. Y. He, R. B. Huan, T. L. Zhao and H. J. Guo, Prevalence of *Helicobacter pylori* infection in China from 2014-2023: A systematic review and meta-analysis, *World J. Gastroenterol.*, 2024, **30**, 4636–4656.

4 M. K. Liu, H. Gao, J. L. Miao, Z. Y. Zhang, L. L. Zheng, F. Li, S. Zhou, Z. R. Zhang, S. X. Li, H. Liu and J. Sun, *Helicobacter pylori* infection in humans and phytotherapy, probiotics, and emerging therapeutic interventions: A review, *Front. Microbiol.*, 2024, **14**, 1330029.

5 H. MØller, E. Heseltine and H. Vainio, Schistosomes, liver flukes and *Helicobacter pylori*, *Int. J. Cancer*, 1995, **60**, 557–589.

6 H. Kishikawa, K. Ojiro, K. Nakamura, T. Katayama, K. Arahata, S. Takarabe, S. Miura, T. Kanai and J. Nishida, Previous *Helicobacter pylori* infection-induced atrophic gastritis: A distinct disease entity in an understudied population without a history of eradication, *Helicobacter*, 2020, **25**, e12669.

7 R. Kataria and A. Khatkar, Lead molecules for targeted urease inhibition: An updated review from 2010-2018, *Curr. Protein Pept. Sci.*, 2019, **20**, 1158–1188.

8 S. Y. Li, Y. Zhang, Y. N. Wang, L. C. Yuan, C. C. Kong, Z. P. Xiao and H. L. Zhu, Identification of (N-aryl-N-arylsulfonyl)aminoacetohydroxamic acids as novel urease inhibitors and the mechanism exploration, *Bioorg. Chem.*, 2023, **130**, 106275.

9 M. Grabarek, W. Tabor, P. Krzyżek, J. Bąkowicz, A. Grabowiecka, Ł. Berlicki and A. Mucha, Synthesis of phosphonate derivatives of benzisoselenazolones and their remarkable antiureolytic activity in *Helicobacter pylori* cells, *J. Med. Chem.*, 2025, **68**, 20324–20339.

10 I. Khan, A. Khan, S. Ahsan Halim, A. Saeed, S. Mehsud, R. Csuk, A. Al-Harrasi and A. Ibrar, Exploring biological efficacy of coumarin clubbed thiazolo[3,2-b][1,2,4]triazoles as efficient inhibitors of urease: A biochemical and *in silico* approach, *Int. J. Biol. Macromol.*, 2020, **142**, 345–354.

11 S. Loharch and Ł. Berlicki, Rational development of bacterial ureases inhibitors, *Chem. Rec.*, 2022, **22**, e202200026.

12 S. Dodla, K. Martin, U. Singh, W. Bible, J. O'Brien, R. Garcia, Z. Tsanglao, J. Andrews and K. Pavuluri, Effects of urea micronized sulfur combined with urease and nitrification inhibitors on nitrogen transformation, losses, and crop response, *Nutr. Cycling Agroecosyst.*, 2025, **131**, 329–346.

13 J. W. Zhang, E. C. Hoedt, Q. Liu, E. Berendsen, J. J. Teh, A. Hamilton, A. W. O' Brien, J. Y. L. Ching, H. Wei, K. Yang, Z. Xu, S. H. Wong, J. W. Y. Mak, J. J. Y. Sung, M. Morrison, J. Yu, M. A. Kamm and S. C. Ng, Elucidation of Proteus mirabilis as a key bacterium in crohn's disease inflammation, *Gastroenterology*, 2021, **160**, 317–330.

14 S. Kunkalienkar, N. S. Gandhi, A. Gupta, M. Saha, A. Pai, S. Shetty, A. Gupta, N. Dhas, R. C. Hariharapura, K. Nandakumar, N. Narasimhaswamy and S. Moorkoth, Targeting urease: A promising adjuvant strategy for effective *Helicobacter pylori* eradication, *ACS Omega*, 2025, **10**, 28643–28669.

15 R. Arora, U. Issar and R. Kakkar, *In Silico* study of the active site of *Helicobacter pylori* urease and its inhibition by hydroxamic acids, *J. Mol. Graph. Model.*, 2018, **83**, 64–73.

16 W. Yang, Q. Q. Feng, Z. Y. Peng and G. C. Wang, An overview on the synthetic urease inhibitors with structure-activity relationship and molecular docking, *Eur. J. Med. Chem.*, 2022, **234**, 114273.

17 O. Güven, E. Menteşe, M. Emirik, B. B. Sökmen and G. Akyüz, Benzimidazolone-piperazine/triazole/thiadiazole/furan/thiophene conjugates: Synthesis, *in vitro* urease inhibition, and *in silico* molecular docking studies, *Arch. Pharm.*, 2023, **356**, e2300336.

18 M. A. Haq, M. Nazir, G. Jabeen, N. Jabeen, S. Naz, H. Nawaz and J. Xu, Inhibitory effect of polyphenols from sumac, pomegranate and Indian almond on urease producing bacteria and jack bean urease activity, *Int. J. Biol. Macromol.*, 2024, **276**, 133735.

19 W. Yang, Z. Peng and G. Wang, An overview: Metal-based inhibitors of urease, *J. Enzyme Inhib. Med. Chem.*, 2023, **38**, 361–375.

20 C. Follmer, Ureases as a target for the treatment of gastric and urinary infections, *J. Clin. Pathol.*, 2010, **63**, 424–430.

21 L. P. S. Viana, L. R. Pinheiro, L. W. Petrillo, I. G. Medeiros, T. G. Rizo, L. V. Modolo, C. M. da Silva and Â. de Fatima, Hydroxamic acids derivatives: Greener synthesis, antiureolytic properties and potential medicinal chemistry applications - A concise review, *Curr. Top. Med. Chem.*, 2025, **25**, 141–161.

22 E. Oner, T. Sahin, I. Demirhan and O. Kilic, Determination of bioactive compounds and biological properties of olive fruit extract (*Olea europaea* L.), *Indian J. Exp. Biol.*, 2025, **63**, 690–702.

23 S. Topuz and M. Bayram, Oleuropein extraction from leaves of three olive varieties (*Olea europaea* L.): Antioxidant and antimicrobial properties of purified oleuropein and oleuropein extracts, *J. Food Process. Pres.*, 2022, **46**, e15697.

24 S. M. Pourtorabi, A. Kaeidi and J. Hassanshahi, Neuroprotective role of oleuropein in post-myocardial

infarction rats: Targeting antioxidant, anti-inflammatory, and anti-apoptotic mechanisms, *Eur. J. Pharmacol.*, 2025, **1003**, 177936.

25 N. Jahan, M. Mandal, I. H. Rakib, M. S. Al Hasan, E. Mia, N. T. Yana, M. Alfaifi, F. H. Altemani, R. Hossan, U. H. Sumaya, A. M. W. Hasan, M. A. Sayeed, M. A. Mou, M. T. Islam and M. S. Bhuia, Oleuropein modulates anti-inflammatory activity of celecoxib and ketoprofen through cyclooxygenase pathway: *In vivo, in silico* and pharmacokinetics approaches, *Naunyn-Schmiedeberg's Arch. Pharmacol.*, 2025, **398**, 16195–16208.

26 M. A. Esfandiary, A. R. Khosravi, S. Asadi, D. Nikaein, J. Hassan and A. Sharifzadeh, Antimicrobial and anti-biofilm properties of oleuropein against *Escherichia coli* and fluconazole-resistant isolates of *Candida albicans* and *Candida glabrata*, *BMC Microbiol.*, 2024, **24**, 154.

27 S. Al-Quraishy, M. S. Othman, M. A. Dkhil and A. E. Abdel Moneim, Olive (*Olea europaea*) leaf methanolic extract prevents HCl/ethanol-induced gastritis in rats by attenuating inflammation and augmenting antioxidant enzyme activities, *Biomed. Pharmacother.*, 2017, **91**, 338–349.

28 A. C. A. Sosa, M. L. Mariani, A. E. Vega and A. B. Penissi, Extra virgin olive oil inhibits *Helicobacter pylori* growth *in vitro* and the development of mice gastric mucosa lesions *in vivo*, *Front. Microbiol.*, 2022, **13**, 961597.

29 J. M. Silvan, E. Guerrero-Hurtado, A. Gutiérrez-Docio, T. Alarcón-Cavero, M. Prodanov and A. J. Martinez-Rodriguez, Olive-leaf extracts modulate inflammation and oxidative stress associated with human *H. pylori* infection, *Antioxidants*, 2021, **10**, 2030.

30 M. Villalva, J. M. Silvan, E. Guerrero-Hurtado, A. Gutierrez-Docio, J. Navarro Del Hierro, T. Alarcón-Cavero, M. Prodanov, D. Martin and A. J. Martinez-Rodriguez, Influence of *in vitro* gastric digestion of olive leaf extracts on their bioactive properties against *H. pylori*, *Foods*, 2022, **11**, 1832.

31 Z. P. Xiao, Z. Y. Peng, J. J. Dong, J. He, H. Ouyang, Y. T. Feng, C. L. Lu, W. Q. Lin, J. X. Wang, Y. P. Xiang and H. L. Zhu, Synthesis, structure-activity relationship analysis and kinetics study of reductive derivatives of flavonoids as *Helicobacter pylori* urease inhibitors, *Eur. J. Med. Chem.*, 2013, **63**, 685–695.

32 C. J. Patton and S. R. Crouch, Spectrophotometric and kinetics investigation of the Berthelot reaction for the determination of ammonia, *Anal. Chem.*, 2002, **49**, 464–469.

33 Q. Lu, Z. S. Zhang, Y. F. Xu, Y. J. Chen and C. L. Li, Sanguinarine, a major alkaloid from *Zanthoxylum nitidum* (Roxb.) DC., inhibits urease of *Helicobacter pylori* and jack bean: Susceptibility and mechanism, *J. Ethnopharmacol.*, 2022, **295**, 115388.

34 J. V. Schloss, Significance of slow-binding enzyme inhibition and its relationship to reaction-intermediate analogs, *Acc. Chem. Res.*, 1988, **21**, 348–353.

35 Q. Lu, J. H. Wang, Y. Tang, W. N. Li and C. L. Li, Phytochemical analysis of dried ginger extract and its inhibitory effect and mechanism on *Helicobacter pylori* and associated ureases, *Food Funct.*, 2025, **16**, 1100–1115.

36 H. Shaalan, M. Azrad and A. Peretz, The effect of three urease inhibitors on *H. pylori* viability, urease activity and urease gene expression, *Front. Microbiol.*, 2024, **15**, 1464484.

37 E. Raoufi, H. Akrami, B. Khansarinejad and H. Abtahi, Expression and antigenic evaluation of *Helicobacter pylori* UreB fragment, *Jundishapur J. Microbiol.*, 2017, **10**, e41645.

38 M. H. Yuen, Y. H. Fong, Y. S. Nim, P. H. Lau and K. B. Wong, Structural insights into how GTP-dependent conformational changes in a metallochaperone UreG facilitate urease maturation, *Proc. Natl. Acad. Sci. USA*, 2017, **114**, E10890–E10898.

39 J. Rückriemen, O. Klemm and T. Henle, Manuka honey (*Leptospermum scoparium*) inhibits jack bean urease activity due to methylglyoxal and dihydroxyacetone, *Food Chem.*, 2017, **230**, 540–546.

40 Y. Tang, F. Yang, X. Wen, Y. Zhou, R. Tang, X. Z. He, Q. Lu and C. L. Li, Component characterization of *Smilax glabra* Roxb., and its inhibitory activity against *Helicobacter pylori* through targeted suppression of its secreted urease, *Front. Cell. Infect. Microbiol.*, 2025, **15**, 1617330.

41 L. Mazzei, U. Contaldo, F. Musiani, M. Cianci, G. Bagnolini, M. Roberti and S. Ciurli, Inhibition of urease, a Ni-enzyme: The reactivity of a key thiol with mono- and di-substituted catechols elucidated by kinetic, structural, and theoretical studies, *Angew. Chem., Int. Ed.*, 2021, **60**, 6029–6035.

42 Q. Lu, D. P. Tan, Y. F. Xu, M. G. Liu, Y. Q. He and C. L. Li, Inactivation of jack bean urease by nitidine chloride from *Zanthoxylum nitidum*: Elucidation of inhibitory efficacy, kinetics and mechanism, *J. Agric. Food Chem.*, 2021, **69**, 13772–13779.

43 K. Takishima, T. Suga and G. Mamiya, The structure of jack bean urease: The complete amino acid sequence, limited proteolysis and reactive cysteine residues, *Eur. J. Biochem.*, 1988, **175**, 151–165.

44 A. Balasubramanian and K. Ponnuraj, Crystal structure of the first plant urease from jack bean: 83 years of journey from its first crystal to molecular structure, *J. Mol. Biol.*, 2010, **400**, 274–283.

45 H. L. Barazorda-Ccahuana, B. Gómez, F. Mas and S. Madurga, Effect of pH on the supramolecular structure of *Helicobacter pylori* urease by molecular dynamics simulations, *Polymers*, 2020, **12**, 2713.

46 Z. Y. Xiong, B. Z. Guo, Y. C. Wei, G. Q. Zhang, L. Wang and Y. N. Chen, Effects of intramolecular proton acceptors located near sulfhydryl groups on sulfhydryl compounds for acrylamide elimination, *Food Chem.*, 2023, **410**, 135476.

47 X. Wang, S. Y. Cheng, C. Y. Liu, Y. Zhang, M. J. Su, X. D. Rong, H. C. Zhu, M. H. Yu, W. L. Sheng and B. C. Zhu, A novel ratiometric fluorescent probe for the detection of nickel ions in the environment and living organisms, *Sci. Total Environ.*, 2022, **840**, 156445.

48 F. Niu, K. X. Yan, L. H. Pang, D. Qu, X. L. Zhao and Z. L. You, Synthesis and structural characterization of Schiff base copper(II) complexes with *Helicobacter pylori* urease inhibitory activities, *Inorg. Chim. Acta*, 2015, **435**, 299–304.

49 E. S. Cunha, X. Chen, M. Sanz-Gaitero, D. J. Mills and H. Luecke, Cryo-EM structure of *Helicobacter pylori* urease

with an inhibitor in the active site at 2.0 Å resolution, *Nat. Commun.*, 2021, **12**, 230.

50 X. D. Yu, R. B. Zheng, J. H. Xie, J. Y. Su, X. Q. Huang, Y. H. Wang, Y. F. Zheng, Z. Z. Mo, X. L. Wu, D. W. Wu, Y. E. Liang, H. F. Zeng, Z. R. Su and P. Huang, Biological evaluation and molecular docking of baicalin and scutellarin as *Helicobacter pylori* urease inhibitors, *J. Ethnopharmacol.*, 2015, **162**, 69–78.

51 Q. Lu, Y. H. Xie, X. F. Wang, H. H. Chen, Y. F. Xu and C. L. Li, Piceatannol, a natural polyphenol from grape, inhibits *Helicobacter pylori* through targeted suppression of its secreted urease, *Food Sci. Nutr.*, 2025, **13**, e70932.

52 X. D. Yu, J. H. Xie, Y. H. Wang, Y. C. Li, Z. Z. Mo, Y. F. Zheng, J. Y. Su, Y. E. Liang, J. Z. Liang, Z. R. Su and P. Huang, Selective antibacterial activity of patchouli alcohol against *Helicobacter pylori* based on inhibition of urease, *Phytother Res.*, 2015, **29**, 67–72.

53 Z. Z. Mo, X. F. Wang, X. Zhang, J. Y. Su, H. M. Chen, Y. H. Liu, Z. B. Zhang, J. H. Xie and Z. R. Su, Andrographolide sodium bisulphite-induced inactivation of urease: Inhibitory potency, kinetics and mechanism, *BMC Complementary Altern. Med.*, 2015, **15**, 238.